

# Characterizing MEMS Switch Reliability for Cryogenic Applications such as Quantum Computing

Peter Bradley<sup>1</sup>, Elizabeth Sorenson<sup>1,2</sup>, Damian Lauria<sup>3</sup> and Li-Anne Liew<sup>1</sup>

<sup>1</sup>Applied Chemicals and Materials Division, National Institute of Standards and Technology, Boulder, CO 80305, USA.

<sup>2</sup>Department of Physics, University of Colorado at Boulder, Boulder, CO 80309, USA

<sup>3</sup>Office of Information Systems Management, National Institute of Standards and Technology, Boulder, CO 80305, USA

Email: Peter.Bradley@nist.gov

**Abstract.** Micro Electromechanical Systems (MEMS) switches offer many advantages over conventional larger switches. One potential application we are exploring is the use of commercial radio frequency (RF) MEMS switches for quantum computing applications. However, it is well-documented that cryogenic temperatures can cause mechanical reliability issues for MEMS. Furthermore, commercial RF MEMS switches are designed for room temperature operation, thus their reliability at cryogenic temperatures is unknown. Commercial MEMS switches are also packaged inside sealed housings, which prevent the use of optical methods for characterization and inspection. We are therefore developing test methods to evaluate the reliability of commercial RF MEMS switches at cryogenic temperatures. We describe our test methods and preliminary reliability test data from room temperature down to 55 K.

## 1. Introduction

Electrostatically actuated RF MEMS (micro electromechanical systems) switches offer many advantages over traditional larger switches, such as smaller size, lower weight and power consumption, faster switching speeds, lower insertion loss, and higher linearity. These advantages make them attractive for many applications ranging from telecommunications to defense. Recent reviews of RF MEMS switch technology and applications can be found in [1, 2]. Another potential use for RF MEMS switches is in quantum computing applications. While there are many qubit technologies, a common denominator is the need for RF signals to initialize, condition, and read out the qubits at cryogenic temperatures. This paper is a product of an interdisciplinary program at NIST focused on developing new cryogenic microwave measurements and calibrations for potentially scaling the number of qubits from  $10^2$  to  $10^6$  to support the commercialization of quantum computing [3].

Since the early 2000's, there has been interest in developing RF MEMS switches for superconducting circuits down to ~1 K. Most of these devices have been academic prototypes that were operated as unpackaged chips, e.g. [4, 5, 6]. A study from 2008 focused on testing *commercial* MEMS switches (from a different vendor than in the present work) at 77 K with the MEMS chip unsealed and directly exposed to the test chamber environment [7]. Another study from 2008 involved flip-chip packaging of RF MEMS switches, but most test data was at room temperature [8]. Commercial devices



offer advantages over laboratory prototypes; however, current commercial MEMS switches are not designed for cryogenic temperatures. Structural damage to the MEMS and packaging can occur due to thermal expansion mismatches and residual stresses during large temperature excursions and thermal cycling. Furthermore, any temperature-dependent change in material properties can also affect device performance. Even if the switch does not catastrophically fail, gradual damage accumulation could occur. Therefore, our goal is to evaluate the reliability of *commercial* RF MEMS switches at cryogenic temperatures when the device is operated outside its intended operating parameters.

## 2. Experimental methods

### 2.1 MEMS switches

The two main classes of RF MEMS switches are the capacitive shunt switch and the DC-contact switch [1, 2]. The DC contact switch is typically a  $\sim 2$   $\mu\text{m}$ -thick metal cantilever beam that bridges a coplanar waveguide (CPW) line that has a break. A separate metal trace under part of the beam acts as a drive electrode for the MEMS. When a DC voltage is applied between this drive electrode and the cantilever, an electrostatic force is created between the two, pulling the beam downwards. At a critical voltage the free end of the beam collapses onto the substrate (but without touching the drive electrode), forming an electrical short between the two ends of the CPW signal line, allowing an RF signal through. When the DC drive voltage is turned off, the beam snaps back up, turning off the switch. Typical drive voltages are on the order of tens of volts; however, commercial MEMS switches include control circuitry allowing a user to input a lower voltage (typically 5 V), which the control circuit then amplifies while isolating it from the RF signal.

We purchased a commercial single pole four throw DC-contact RF MEMS switch. The MEMS is sealed inside a chip package housing (MEMS packages typically contain a rough vacuum) that is mounted onto a printed circuit board (PCB) with standard SMA terminations for RF cables. The PCB has one common RF ground line and four RF signal lines corresponding to the four MEMS switches inside the package. The device manufacturer provided a separate PCB with the drive voltage-amplification circuitry; however, we did not use this control board but instead directly applied the drive voltage to the MEMS from a high-voltage DC power supply, in order to have more direct control over the drive voltages.

The MEMS manufacturer's specification sheet states that the lowest recommended operating temperature and storage temperature are  $-40$   $^{\circ}\text{C}$  (233 K) and  $-65$   $^{\circ}\text{C}$  (208 K), respectively, and that the MEMS is not intended for hot switching (where the switch is turned on and off while conducting RF signals). However, in quantum computing applications the MEMS switch will be required to operate at much lower temperatures and potentially while hot switching. Thus, while the manufacturer's data sheet specifies a lifetime of  $3 \times 10^9$  cycles, the reliability is unknown for cryogenic applications, which are far outside the manufacturer's recommended operating conditions.

### 2.2 Cryostat test set up

Since commercial MEMS switches are sealed inside package housings, optical methods often used for MEMS characterization are not feasible. Therefore, we used electrical tests that are described in the Results section. Figure 1 shows the test apparatus we constructed, by repurposing and adapting a pre-existing system previously employed to evaluate heat transfer coefficients in microchannels [9, 10, 11], to test the MEMS from room temperature down to a target of 12 K. The apparatus consists of a Gifford-McMahon (GM) cryocooler and vacuum chamber instrumented with electrical feedthroughs and temperature feedthroughs, electronics for temperature measurement and control, electronics for driving and characterizing the MEMS, and software to run the tests and acquire the data.

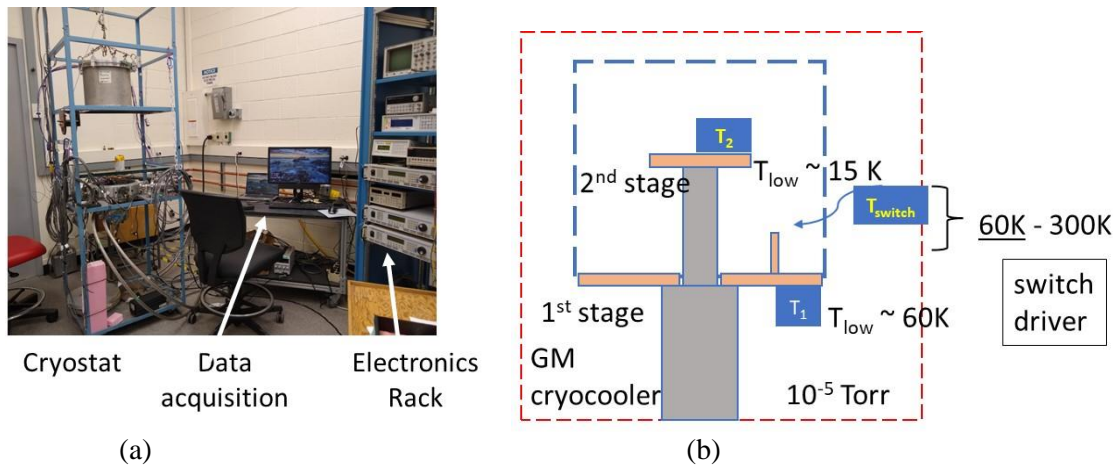


**Figure 1.** (a) Photograph of the cryogenic MEMS test set up: cryostat, electronics for temperature control/monitoring and MEMS testing, data acquisition system. (b) Schematic of the cryostat.

Figure 2 shows photographs of the MEMS PCB in the vacuum chamber. We clamped the MEMS board to a copper adapter, using screws to adjust the applied force. Type-E thermocouples were attached with cyanoacrylate glue to the top of the chip package, the PCB, the thermal adapter under the PCB, and the cryostat's cooling plate under the adapter. This mounting approach is designed to maximize thermal conduction to the MEMS while providing electrical isolation and allowing for debonding. Insulated wires were soldered from the PCB and connected to the vacuum chamber's electrical feedthroughs to provide the drive voltage.

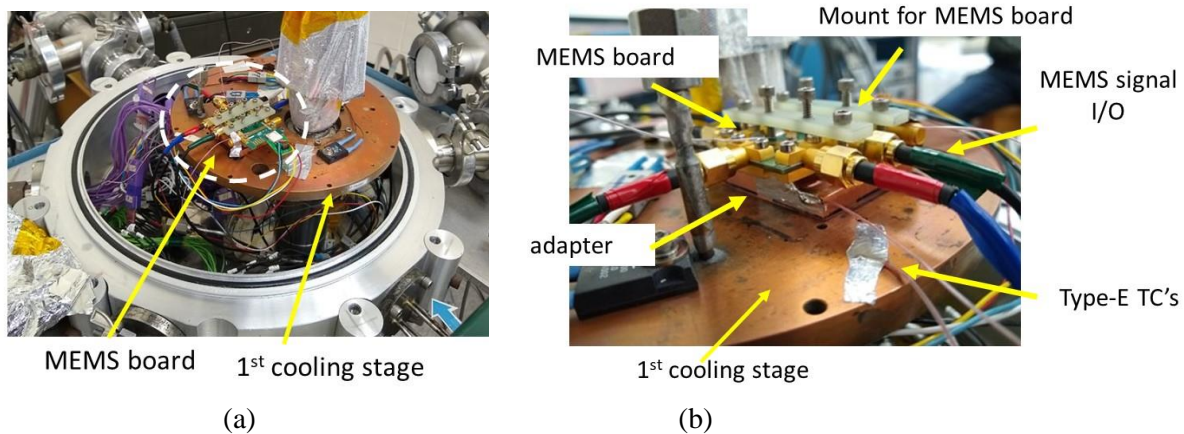


**Figure 2.** Close-up photographs of the cryogenic chamber: (a) Top view of the cooling stage with MEMS board mounted. (b) Side view of MEMS board mounted on the cooling stage.

The MEMS PCB contains four SMA (coaxial RF connectors) terminations for signal I/O. SMA cables connected the PCB to SMA feedthroughs on the vacuum chamber. Outside the chamber, SMA-to-BNC adapters connected BNC cables between the chamber and the electronics rack. Even though the MEMS will be switching RF signals in quantum computing applications, we used low-frequency and DC test signals for our hot-switching tests as these provide more direct information on the MEMS mechanical reliability. For cold-switching tests we measured the MEMS contact resistance using a four-probe configuration to remove the lead resistance. We developed programs, using commercial software, to acquire and plot the data and are currently adding temperature control and automation capability.

The cryostat was pumped to a pressure of  $0.00133\text{ Pa}$  ( $1 \times 10^{-5}\text{ Torr}$ ). The chamber has two cooling stages as shown above in Fig 1(b). Each cooling stage has two heaters for temperature control. The

second stage reached 12 K but in these preliminary MEMS tests we used only the first cooling stage, which reached a minimum of 55 K. Load mapping of the stages was conducted prior to installation of the MEMS as shown in Figure 3(a) and (b), indicating how to achieve targeted 2<sup>nd</sup> stage temperatures given 1<sup>st</sup> stage temperatures and loads. Figure 4 shows the measured steady state temperatures of the MEMS chip package, PCB, and the adapter, at each steady state stage temperature.

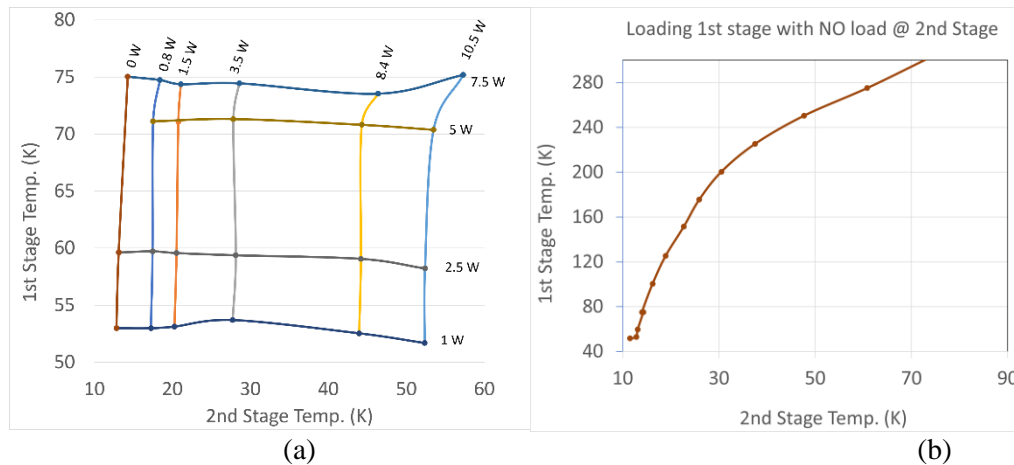


**Figure 3.** Load maps for the two-stage GM apparatus. (a) Characterizing both stages. (b) Loading 1<sup>st</sup> stage from 55 K to 300 K to obtain set corresponding loads for temperature set points for the MEMS testing.

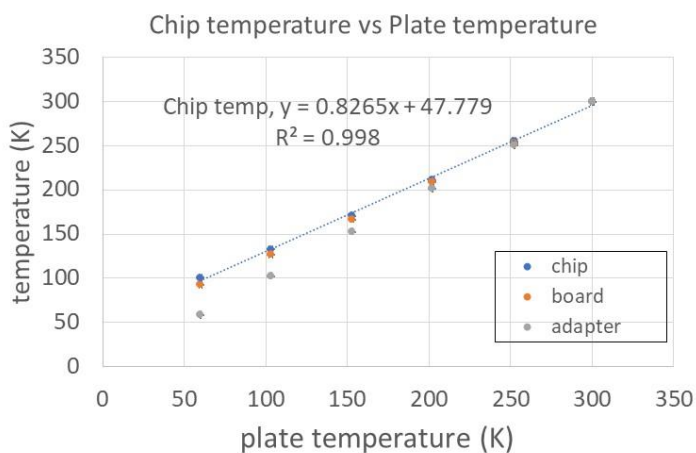


**Figure 4.** Measured steady state temperatures of the top of the MEMS chip package ("chip"), the PCB that the chip package is mounted on ("board"), and the copper adapter that the board is mounted on, versus the measured temperature of the cryostat's cold stage ("plate").

### 3. Experimental results

#### 3.1 Test protocols and initial tests at room temperature

It is well-documented that when MEMS electrostatic actuators are operated to the pull-in condition they exhibit hysteresis in their voltage-displacement relationship [1, 2]. Hysteresis is not a concern for switch end-users since they will operate the switch by simply turning it on at the full drive voltage and off at 0 V. However, to evaluate the switch reliability we examined the hysteresis as this will be a more sensitive measure of temperature-induced changes and damage accumulation.

Figure 5(a) shows three hysteresis curves corresponding to three tests of the same MEMS switch at room temperature, during hot-switching tests with a 1 VDC input test signal. Figure 5(b) shows the same device in three cold-switching tests at room temperature, whereby instead of inputting a test signal we measured the contact resistance of the switch using a four-probe configuration. Initially the MEMS cantilever's free end was suspended over the substrate so that there was no output

test signal detected (hot switching test) and the contact resistance is infinite (in Fig 5b we use an arbitrary value of  $3\ \Omega$  for plotting purposes). When the drive voltage  $V_d$  is gradually increased in increments of 1 V, at a critical  $V_d$  the cantilever's free end pulls down, making an initial ohmic contact with the CPW line and conducting the 1 V test signal. As  $V_d$  is further increased, the contact force is increased leading to a minimum in contact resistance. When  $V_d$  is gradually decreased in 1 V increments, the critical  $V_d$  at which the switch releases (or “pulls up”) is lower than that at which it pulled down. When the same MEMS switch is tested multiple times, variations are observed in the hysteresis curves. The measurement uncertainties in the voltage, contact resistance, and temperature were 0.1 V, 0.001 Ohm, and 0.1 K, respectively.

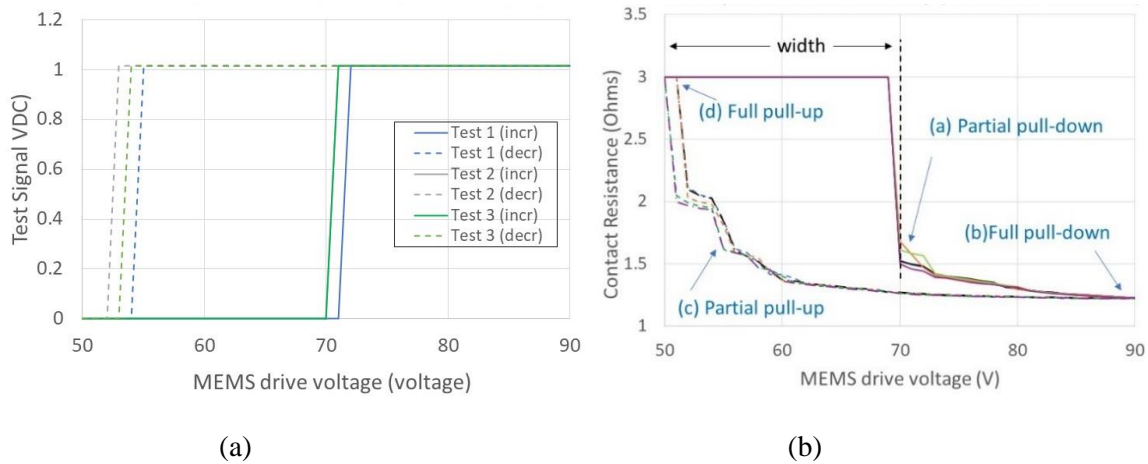


**Figure 5.** Room temperature hysteresis of one commercial DC-contact MEMS switch. The solid lines indicate increasing drive voltage, and the dashed lines indicate decreasing drive voltage. (a) Hot switching with a 1 Vdc test signal. (b) Cold switching. In (b) the initial contact resistance is infinite; we use an arbitrary value of  $3\ \Omega$  only to provide clarity in the plot.

Figure 6 shows what we call a “creep” test at room temperature. In this cold-switching test, we actuated the MEMS switch at 90 V, to ensure firm ohmic contact, and left the switch in the “on” position for an hour while measuring the contact resistance once per minute. As shown in Fig 6, when the switch was tested multiple times, the initial contact resistance varied, but the trend of decreasing resistance over time as the switch is held down is repeatable. Brown et al [7] did similar tests on their commercial (from a different manufacturer) but unsealed MEMS switches at room temperature and 77 K and found similar room-temperature behavior as seen in Fig 6. A significant difference between their tests and ours is that their MEMS chips were unpackaged and thus intentionally subjected to the gas type and pressure inside their test chamber.

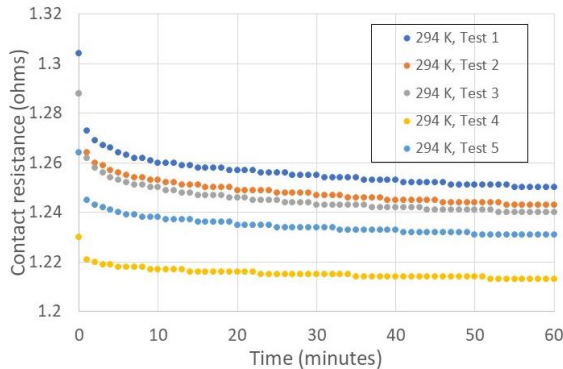


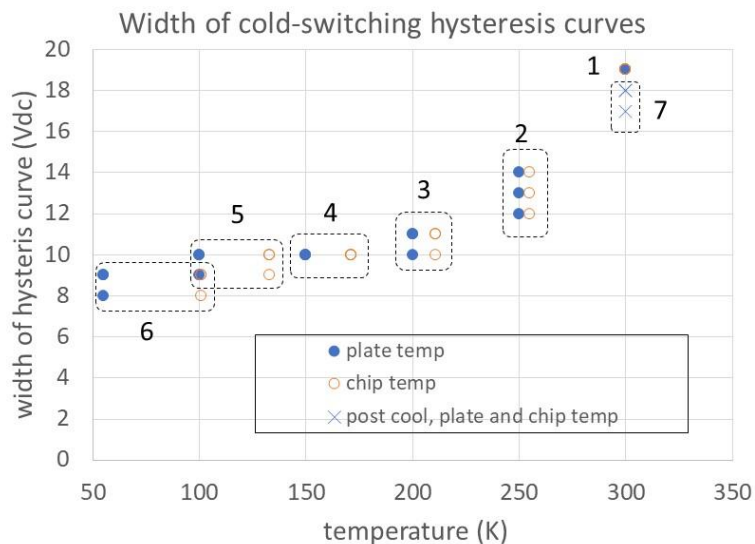
**Figure 6.** Room-temperature “creep” tests of a MEMS switch at room temperature.



### 3.2 Tests at cryogenic temperatures

Figs 5 and 6 above show the baseline characteristics we measured for a single MEMS switch at room temperature. We then gradually cooled the MEMS in stages down to  $\sim 55$  K and repeated the above tests at intermediate steady-state temperatures. We repeated each test three times per temperature. After the lowest temperature tests were completed, the GM cryocooler was turned off and the test system was allowed to gradually warm up to room temperature. After two weeks another set of tests at room temperature was done, to compare with the pre-cooled room-temperature tests.

Figure 7 shows the width of the hysteresis curves at each temperature, during cold switching. The hot-switching tests produced similar results. The hysteresis width decreased with decreasing temperature, with the most significant reduction occurring between room temperature and 250 K, which is within the MEMS operating range stated in the manufacturer's data sheet. Fig 7 also shows that the post-cooling room-temperature hysteresis width is  $\sim 10\%$  lower than the pre-cooling width. As noted by Brown et al [7], a difference between the pre- and post-cooling actuation voltages would indicate a permanent deformation in the MEMS structure.



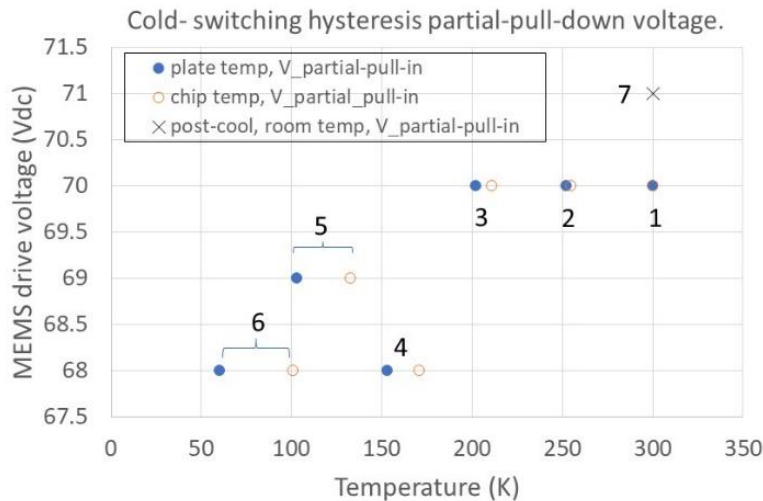
**Figure 7.** Width of the MEMS hysteresis curve, during cold switching, as the chip and plate were cooled from room temperature to  $\sim 55$  K. Three tests were performed at each steady state temperature, shown grouped and numbered in order of when the measurements were taken. The post-cooling tests were done at room temperature two weeks after the 55 K tests. The standard deviation in width at each temperature is  $\sim 0.6$  V. The width vs. temperature plot for the hot-switching tests is similar.

Figure 8 shows the measured partial pull-in voltage of the MEMS switch as a function of the plate and chip temperatures. We define the “partial pull-in/down” as the voltage at which the contact resistance first becomes non-infinite, to distinguish from the “full pull-in/down” voltage where the contact resistance has reached a minimum and the switch is considered to be “on”, as shown in Fig 5b.

We found the full pull-in voltage to be constant (90 V) with temperature. But from Fig 8, a trend emerges of decreasing *partial* pull-in voltage with decreasing temperature. This is opposite to the literature on DC contact RF MEMS switches, which show *increasing* pull-in voltage with decreasing temperature due to material stiffening and/or CTE mismatch stresses in the device [4, 5, 6]. Gong et al [5] measured the pull-in and pull-up voltages of their MEMS switches and reported a  $\sim 55\%$  increase in both, between room temperature and 1.6 K. Other researchers also report the trend of *increasing* pull-in voltage with decreasing temperature [4, 6], which is the opposite trend to what is seen in Fig 8. Furthermore, our observed decrease in pull-in voltage is less than 5 %, whereas in the literature the reported increases ranged from 55 % at 1.6 K [5] to a factor of two at 4 K [6]. (The devices in the literature were unpackaged and all differed in materials, fabrication processes, and design, so there could be many factors accounting for these differences.)

Fig 8 also shows that at post-cooling, our partial pull-in voltage at room temperature is now higher than it was before cooling. The difference is only 1 volt (71 V instead of 70 V), which can be considered negligible; however, considering that this is only one cooling cycle to 55 K, it remains to be seen if further cooling cycles or cooling to lower temperatures will increase these shifts. To our knowledge, the present study is the first to examine the change in hysteresis of commercial fully packaged MEMS at

cryogenic temperatures and the effect of cryogenic cooling on subsequent room-temperature characteristics.



**Figure 8.** MEMS pull-in voltage as the chip and plate are cooled from room temperature to ~ 55 K. Three tests were done at each steady-state temperature. The standard deviations in the voltages at each temperature ranged from 0 – 1 V. The post-cooling tests were done at room temperature two weeks after the cryogenic tests. The numbers indicate the order in which the measurements were taken.

Figure 9 shows the initial and final contact resistances in the creep tests at each steady-state temperature. Note that at 150 K the trend reverses direction. Also, the standard deviation is largest at 150 K, thus suggesting that this temperature is associated with an instability or transition, perhaps related to the materials in the MEMS or its package. Nevertheless, the post-cooling initial and final contact resistances at room temperature return within 0.06 Ohms (for initial resistance) and 0.02 Ohms (for final resistance) of their pre-cooled values, a trend which is qualitatively similar to that reported by Brown et al [7] after cooling to 77 K.

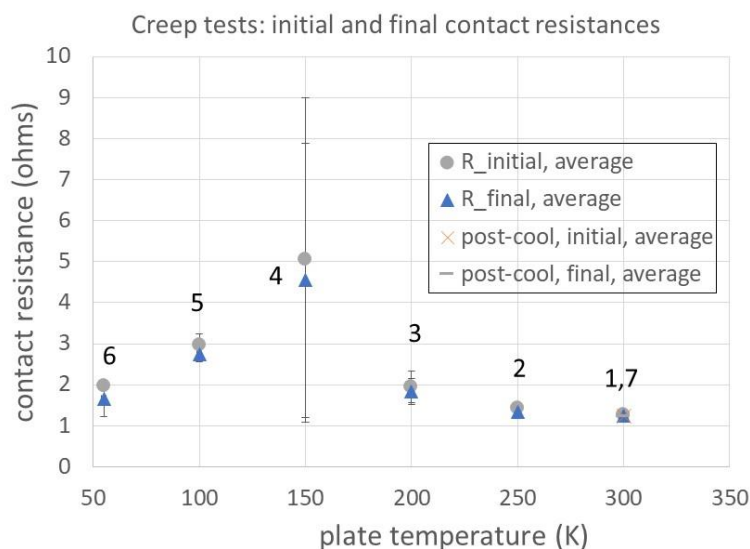


**Figure 9.** Creep test initial and final contact resistances as a function of the stage temperature. The error bars are the standard deviation, with three tests per temperature. The numbers indicate the order in which the measurements were taken. The post-cooling tests were done at room temperature two weeks after the cryogenic tests.

#### 4. Summary

We developed test methods to investigate the mechanical reliability at cryogenic temperatures of commercial fully packaged and sealed DC contact MEMS switches originally intended for room temperature operation. Preliminary tests from room temperature down to 55 K show that the MEMS pull-in voltage decreased by 3 % with decreasing temperature, which is the opposite of trends reported in the literature for unpackaged DC contact MEMS switches. The width of the hysteresis curve

decreased by up to 55 % with decreasing temperature, with the most significant change occurring between room temperature and 250 K. “Creep” tests, whereby the switch was held in the “on” position for an hour and its contact resistance measured over time, showed increasing initial and final contact resistances when the stage was cooled from room temperature to 150 K, after which the trend reversed with decreasing initial and final contact resistance from 150 K to 55 K. Post-cooling tests at room temperature showed no change compared to pre-cooling for the creep tests. But reduction in the hysteresis curve widths and a slight increase in the pull-in voltage, outside of measurement uncertainty, compared to pre-cooling was observed, thus indicating some permanent change in the MEMS has occurred from a single cooling cycle from room temperature to 55 K. Future work will include measuring the switching speed and lowering the test temperature to 12 K which is the limit of the cryostat.

## 5. References

- [1] Tian W, Li P and Yuan L 2018 Research and analysis of MEMS switches in different frequency bands *Micromachines*. **9** 185
- [2] Kurmendra and Kumar R 2021 A review on RF micro-electro-mechanical-systems (MEMS) switch for radio frequency applications *Microsystem Tech.* **27** 2525-42
- [3] Hopkins P, Castellanos-Beltran M, Biesecker J, Brevik J, Dresselhaus P, Fox A, Howe L, Olaya D, Sirois A, Boaventura A, Williams D and Benz S 2022 Measurement challenges for scaling superconductor-based quantum computers *Proc. Int. Conf. Frontiers of Characterization and Metrology for Nanoelectronics (FCMN 2022)*. Monterey, CA June 20-23, 2022
- [4] Noel J, Bogozi A, Vlasov Y and Larkins G 2008 Cryogenic pull-down voltage of microelectromechanical switches *J. MEMS*. **17** (2) 351-55
- [5] Gong S, Shen H and Barker N 2009 Study of broadband cryogenic DC-contact RF MEMS switches *IEEE Trans. Microwave Theory and Techniques*. **57** (2) 3442-49
- [6] Attar S and Masnour R 2015 Integration of niobium low-temperature-superconducting RF circuits with gold-based RF MEMS switches *IEEE Trans. App. Superconductivity*. **25** (3) 1500206
- [7] Brown C, Morris A, Kingon A and Krim J 2008 Cryogenic performance of RF MEMS switch contacts *J. MEMS*. **17** (6) 1460-67
- [8] Muldavin J, Bozler C, Rabe S, Wyatt P and Keast C 2008 Wafer-scale packaged RF microelectromechanical switches *IEEE Trans. Microwave Theory and Techniques*. **56** (2) 522-29
- [9] Baek S and Bradley PE. 2015 Single-phase ambient and cryogenic temperature heat transfer coefficients in microchannels. *IOP Conference Series: Materials Science and Engineering*. **101** 012005.
- [10] Baek S, Bradley PE and Radebaugh R. 2018 Heat transfer coefficient measurement of LN2 and GN2 in a microchannel at low Reynolds flow, *International Journal of Heat and Mass Transfer*. **127** 222-33.
- [11] Baek S, Radebaugh R and Bradley PE. 2020 A new method for heat transfer coefficient measurements of single-phase fluids during laminar flow in microchannels. *International Journal of Heat and Mass Transfer*. **157** 119891.

## Acknowledgments

We thank Andy Slifka and Dylan Williams at NIST for valuable discussions. Specific commercial equipment, instruments, and materials that are identified in this report are listed in order to adequately describe the experimental procedure and are not intended to imply endorsement or recommendation by the National Institute of Standards and Technology.